

# Improved Modeling and Fabrication Techniques for Capacitive Micromachined Ultrasonic Lamb Wave Transducers

Mohammed H. Badi, Goksen G. Yaralioglu, A. Sanlı Ergun, Yongli Huang, and B.T. Khuri-Yakub

Ginzton Laboratory, Stanford University, Stanford, CA 94305-4088, USA

*Abstract*—This paper discusses improvements in the theoretical and experimental framework of Capacitive Micromachined Ultrasonic Lamb Wave Transducers. Theoretically, a new method for the analysis of these Lamb wave devices is proposed using the electro-mechanical capabilities of ANSYS, a commercial finite element package. The model used in these simulations has been verified by comparing its predictions when configured as a clamped transducer to those predicted by the standard equivalent circuit model; the input impedances obtained using the two methods agree to within 1%. This method performs harmonic and transient analyses to predict device performance metrics in the presence of electrostatic forces. Experimentally, this paper introduces a new manufacturing process for the fabrication of Lamb wave devices using CMUT wafer bonding technology. Devices have successfully been built using this technique and preliminary results show significantly improved uniformity in membrane to membrane performance and successful Lamb wave propagation between transducers. The membranes fabricated are 1 cm long and 60  $\mu\text{m}$  wide and have an insertion loss of 16.2 dB near 2.6 MHz.

## I. INTRODUCTION

This paper presents progress made on a new method to excite and detect Lamb waves using the Capacitive Micromachined Ultrasonic Transducer (CMUT). As shown in Figure 1, the devices that are described use high aspect ratio rectangular membranes. As most CMUTs are made from nearly circular membranes, this shape change necessitates a different formulation of the lumped equivalent circuit model used to describe the behaviour of the transducers. A derivation of this model and the equations that accompany it can be found in [1]. Also therein is a description of the sacrificial layer method of manufacturing CMUTs and shows experimental results that were used to confirm the validity of the presented theory. This paper builds on that work by describing more powerful methods of manufacturing and modeling CMUTs. In the former electro-mechanical elements are coupled with purely mechanical ones to predict device behaviour as a function of ac and dc voltages; in the latter wafer-bonding is used which results in higher membrane yield and repeatability.

## II. LAMB WAVES USING CMUTS

Figure 1 presents the high aspect ratio rectangular CMUTs used for the devices described in this paper. An aluminum electrode covers half of the top surface of the membrane and acts as one of the capacitor's electrodes. The other electrode, not shown on the figure, is a thin highly doped region on the top of the silicon surface. When an AC voltage is superimposed on a DC bias and applied between the two electrodes, the membrane will vibrate with a resonant characteristic determined by the geometry of the

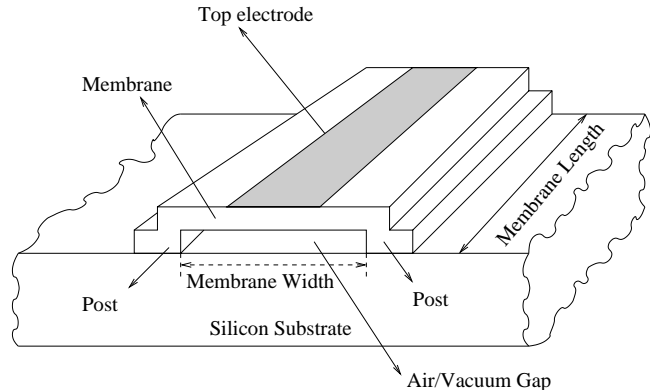


Fig. 1. Diagram of a single CMUT membrane.

structure. Energy from this vibration then couples through the posts shown in Fig. 1 to excite Lamb waves in the silicon plate. While both of the zero order modes are excited in the substrate, the dominant mode that propagates is the lowest-order antisymmetric flexural wave  $A_0$ . Due to the large aspect ratio of the membranes, the wave propagation can be approximated as a plane wave away from the membrane in the lateral direction. The Lamb waves are sensed further down the substrate by an identical receiving membrane. A successful Lamb wave device is efficient in coupling energy from the vibrating membrane to the substrate. As shown in Fig. 2, the energy sink presented by the substrate can be represented in an equivalent circuit model by its highly dissipative resistance  $R_{substrate}$ . Significant coupling will result when this resistance is much greater than that of other dissipative elements in the circuit. Since the membrane impedance  $Z_{mem}$  is reactive, the impedance of air  $Z_{rad}$  is the only other such element in this particular model, and it cannot easily be changed as it is primarily a function of physical constants. Finite Element Analysis shows that this impedance increases with thinner substrate thickness. This finding is consistent with the design of other Lamb wave devices described in the literature that have substrate thickness much smaller than the ultrasonic wavelength [2].

It should be noted that the Lamb wave devices recently built using CMUT technology employed a single membrane at both the transmitter and receiver. This is in contrast to previous such devices as well as those that use other methods to excite the wave. The band shape of the Lamb wave is determined by the CMUT resonance rather than the interplay between the membrane fingers.

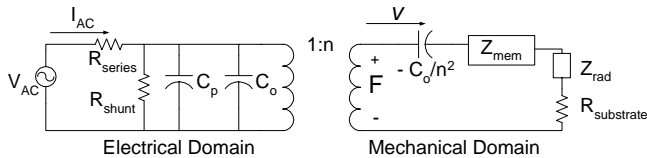


Fig. 2. Equivalent circuit model of a transmitting CMUT.

### III. MODELING

#### A. Verification Of The Finite Element Model

This section verifies that the Finite Element Model<sup>1</sup> properly models the electro-mechanical interactions of a transducer. This verification is done by building a piston in a lossless environment and comparing the input impedance of the resulting structure to that predicted by the equivalent circuit model shown in Fig. 2. The element types used in ANSYS are Plane82 and Trans126.

The first step in the verification process is to confirm that the membrane impedance derived from first principles is correct. The graph in Figure 3 shows the membrane impedance as predicted by finite element analysis (solid) and the equations presented in [1] (dashed). Note that the agreement between the two curves improves as the as the frequency of operation increases. This improvement can be understood by considering the LC model of a mechanical membrane. At higher frequencies the inductor dominates the membrane impedance; this inductor represents the mass of the membrane which can be accurately modeled in both finite element analysis and first order equations. The capacitor which dominates at lower frequencies, on the other hand, represents the spring constant of the membrane. This value of this constant is a strong function of the forces that are used to create the membrane displacement. These forces are difficult to properly model

<sup>1</sup>Finite Element Analysis was performed using ANSYS 5.7

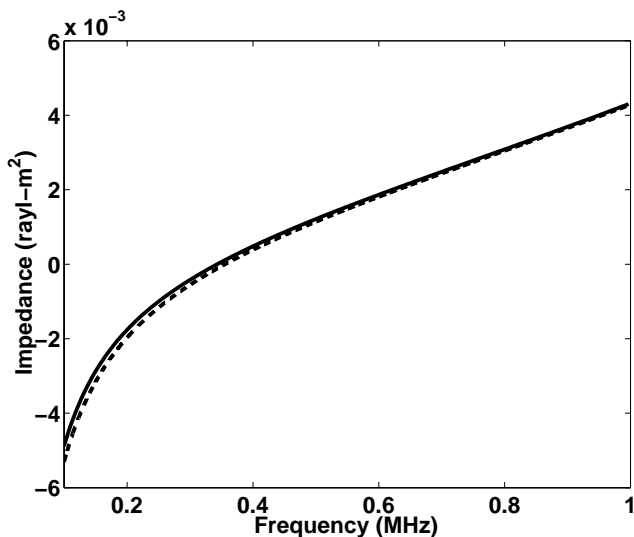


Fig. 3. Membrane impedance as predicted by finite element analysis (solid) and analytical equations (dashed).

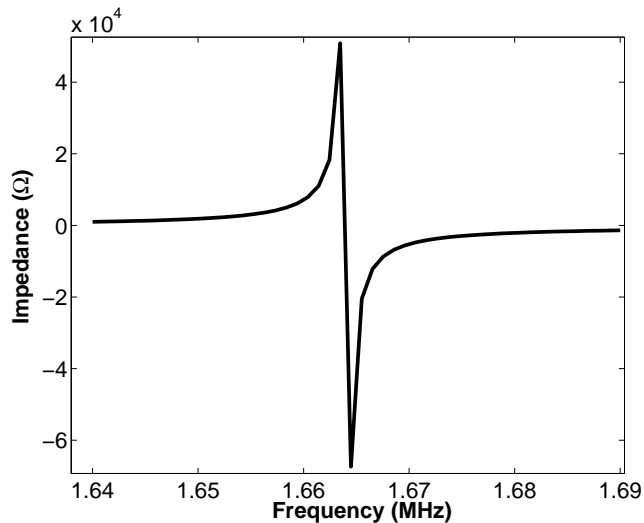


Fig. 4. Input impedance results from finite element and analytical calculations. Due to the fact that both methods result in the same plot, only one curve is discernible in the figure.

analytically.

The device capacitance and transformer ratio equations used are that of the basic parallel plate model [3]. Furthermore, since the CMUT is in a lossless environment,  $R_{series}$ ,  $R_{shunt}$ ,  $Z_{rad}$ , and  $R_{substrate}$  can be ignored.

The input impedance calculated from the equivalent circuit model and finite element analysis are presented in Fig. 4. In the area around resonance the two curves match perfectly lending credence to the finite element model used to analyze the CMUT. Note that the curves match so well that they cannot be discerned from one another in the graph. Only the imaginary part is shown as the real part is equal to zero.

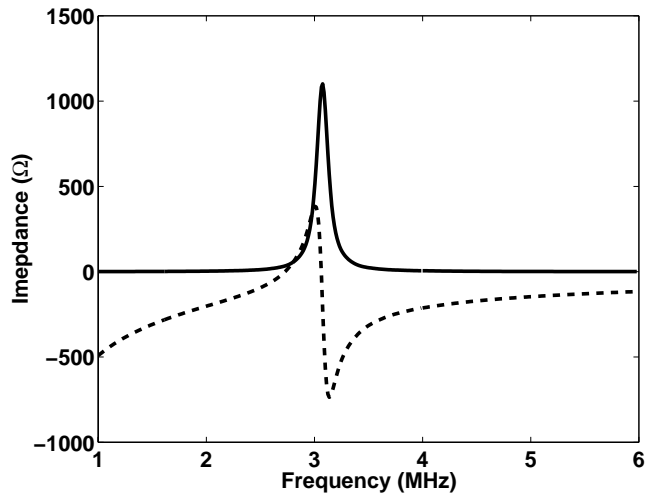


Fig. 5. Input impedance of a CMUT on an 8  $\mu\text{m}$  substrate from finite element calculations. The membrane width was 60  $\mu\text{m}$ , the membrane was 1.34  $\mu\text{m}$  thick, and the gap was .97  $\mu\text{m}$ . The solid and dashed lines represent the real and imaginary parts, respectively.

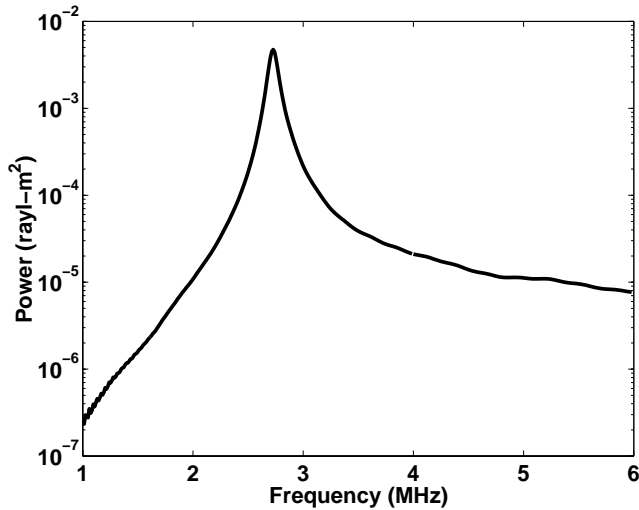


Fig. 6. Power in the  $A_0$  mode of a Lamb wave propagating in an  $8 \mu\text{m}$  substrate as determined from finite element analysis.

### B. Modeling the Lamb Wave Transducer

Having verified the ability of the model to describe the behaviour of a clamped CMUT, the next step is to include losses and its distributed nature. As such the transducer is placed onto a substrate and the forced piston condition is removed. The results in Fig. 5 and Fig. 6 show the curves obtained from finite element analysis (FEA) in a harmonic simulation. The structure in this simulation consists of a  $60 \mu\text{m}$  wide membrane on an  $8 \mu\text{m}$  substrate, representative of the devices actually built. The applied voltage is  $140 \text{ V}$ , approximately one-half of the collapse voltage.

The finite element model can also be used for an electro-mechanical transient analysis. The graph in Fig. 7 represents the result of a transient analysis where a  $.5 \mu\text{s}$  pulse is superimposed on a DC bias and placed at the input of the transmitting CMUT. The electrical energy is converted to a Lamb wave which propagates along the substrate to

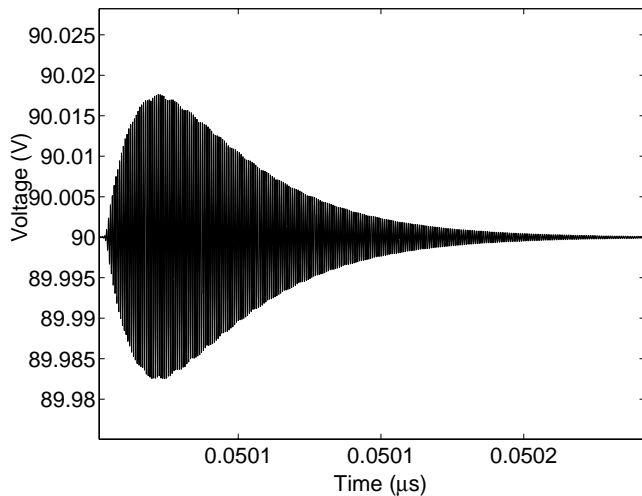


Fig. 7. Signal at the receiving CMUT as determined by a transient finite element analysis. Note that the DC voltage on the MUT is  $90 \text{ V}$ .

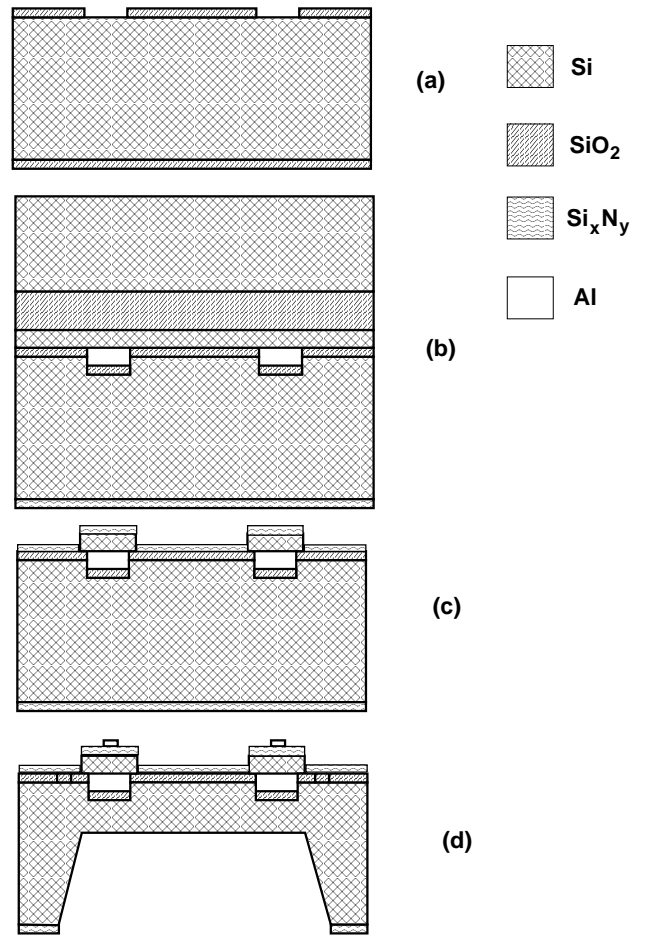


Fig. 8. Input impedance results from finite element and analytical calculations. Due to the fact that both methods result in the same plot, only one graph is discernable in the figure.

a receive membrane where the energy is converted back into its original electrical form; a matching network is in place at both ports. This analysis cannot be done using the harmonic method because the *PSTRES* option in ANSYS does not support the electrical elements needed for the matching network.

## IV. DEVICE FABRICATION

The new manufacturing process used to create these Lamb wave devices relies on the wafer bonding method [4]. Problems with the older sacrificial-layer method include poor control of membrane stress (and therefore performance) and low membrane yield. In this newer process the membrane is made from single crystal silicon. In addition to solving stress and yield problems, this method also significantly decreases the time needed to fabricate a set of devices.

A brief outline of the process is shown in Fig. 8. The first step is to etch a trench into a double-side polished wafer and to follow that with an oxide growth that will act as the device insulation layer (Fig. 8a). An SOI wafer is then bonded to the first wafer and silicon nitride is deposited (Fig. 8b), followed by the removal of the SOI handle

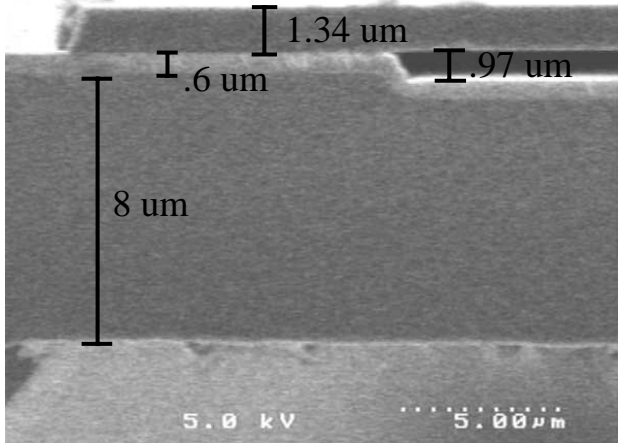


Fig. 9. SEM of a fabricated wafer-bonded CMUT. The thickness of the silicon nitride layer, not visible above, is 500 Å.

and box. The CMUT membranes are then defined by patterning the SOI device layer (Fig. 8c) and silicon nitride is again deposited on both sides. The metallization and back-side etching steps complete the process (Fig. 8d). The etch is performed using a solution of TMAH doped with silicon and ammonium persulfate [5]. An SEM of the resulting device is shown in Fig. 9.

## V. EXPERIMENTAL RESULTS

The input impedance of the two membranes that make up the Lamb wave device is shown in Fig. 10. Note that the curves are similar in shape and amplitude. This agreement is a virtue of the uniformity allowed by wafer bonding. The insertion loss of the device, shown in Fig. 11, is approximately 16.2 dB near 2.6 MHz.

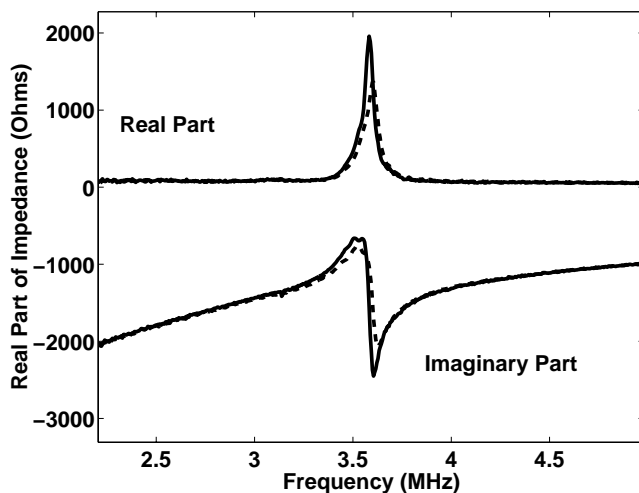


Fig. 10. Input impedances of two membranes that make up a single Lamb wave transducer. Data was obtained using the HP8751A vector network analyzer.

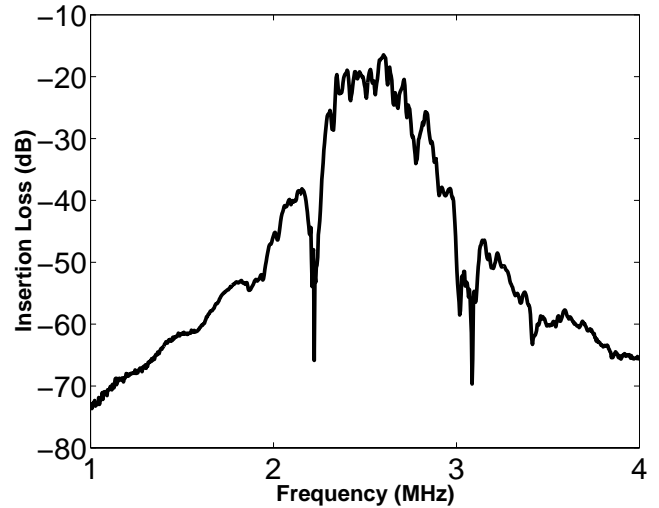


Fig. 11. Insertion loss of the Lamb wave transducer. At 2.6 MHz IL=16.2 dB. Data was obtained using the HP8751A vector network analyzer.

## VI. CONCLUSION

The improvements in the Capacitive Micromachined Ultrasonic Lamb Wave Transducer described in this paper revolve around the modeling work done using the electro-mechanical capabilities of ANSYS 5.7 and the wafer-bonding method of CMUT fabrication. The former helps to give insight in the device behaviour by providing data that includes the effect of electrostatic fields. The latter results in devices with improved uniformity, higher yield, and ease of fabrication. The fabricated structure, built on an 8 μm membrane, has an insertion loss of 16.2 dB near 2.6 MHz.

## REFERENCES

- [1] Mohammed H. Badi, G.G. Yaralioglu, A.S. Ergun, S.T. Hansen, E.J. Wong, and B.T. Khuri-Yakub, "Capacitive micromachined ultrasonic lamb wave transducers using rectangular membranes," *IEEE Transactions on Ultrasonics, Ferroelectrics and Frequency Control*, vol. 50, no. 9, pp. 1191 – 1203, September 2003.
- [2] S.W. Wenzel and R.M. White, "A multisensor employing an ultrasonic lamb-wave oscillator," *IEEE Transactions on Electron Devices*, vol. 35, no. 6, pp. 735 – 43, June 1988.
- [3] F.V. Hunt, *Electroacoustics*, Acoustical Society of America, 1982.
- [4] Yongli Huang, A.S. Ergun, E. Haeggstrom, M.H. Badi, and B.T. Khuri-Yakub, "Fabricating capacitive micromachined ultrasonic transducers with wafer-bonding technology," *Journal of Microelectromechanical Systems*, vol. 12, no. 2, pp. 128 – 37, April 2003.
- [5] Guizhen Yan, P.C.H. Chan, I-Ming Hsing, R.K. Sharma, J.K.O. Sin, and Yangyuan Wang, "An improved tmah si-etching solution without attacking exposed aluminum.," *Sensors and Actuators A (Physical)*, vol. A89, no. 1-2, pp. 135 – 41, March 2001.